Effect of scale deposits on the internal surfaces of the tubes on the superheater operation

MARCIN TROJAN
JAN TALER[*]

Cracow University of Technology, Institute of Thermal Power Engineering, Jana Pawła II 37, 31-864 Kraków, Poland

Abstract A mathematical model of the steam superheater exchanger with distributed parameters has been developed. Scale deposits were assumed to be present on the internal tube surfaces. It was assumed that the inner tube surfaces are covered by a thin layer of scale deposits. The finite volume method was used to solve partial differential equations describing flue gas, tube wall and steam temperature. The developed modeling technique can especially be used for modeling tube heat exchangers when detail information on the tube wall temperature distribution is needed. The numerical model of the superheater developed in the paper can be used for modeling of the superheaters with complex flow arrangement accounting scales on the internal tube surfaces. Using the model proposed the detailed steam, wall and flue gas temperature distribution over the entire superheater can be determined. The steam pressure distribution along its path flow and the total heat transfer rate can also be obtained. The calculations showed that the presence of scale on the internal surfaces of the tubes cause the steam temperature decrease and the heat flow rate transferred from the flue gas to the steam. Scale deposits on the inner surfaces of the tubes cause the tube wall temperature growth and can lead to premature wear of tubes due to overheating.

Keywords: Steam superheater; Scale deposit; Heat exchanger numerical model

---

[*]Corresponding Author. E-mail: taler@mech.pk.edu.pl

Nomenclature

d_h – hydraulic diameter of the superheater tube (for a circular tube, this equals the inner diameter of the tube), m

h_e – equivalent heat transfer coefficient, W/m²K

h_g – heat transfer coefficient on the flue gas side, W/m²K

h_s – heat transfer coefficient at the inner tube surface, W/m²K

k_a – ash deposit thermal conductivity, W/mK

k_s – iron oxides or scales thermal conductivity, W/mK

k_w – tube material thermal conductivity, W/mK

L_r – tube length, m

$\dot{m}_s$ – steam mass flow rate, kg/s

N – number of finite volumes on the tube length

p – static pressure, Pa

r – radius, m

r_a – outer radius of deposit layer, m

r_{in} – inner radius, m

r_o – outer radius, m

s – coordinate along the flow path in direction of flow, m

s_1 – longitudinal pitch perpendicular to the flue gas flow direction, m

s_2 – longitudinal pitch parallel to the flu gas flow direction, m

T_a – deposit layer temperature °C

T_g – flue gas temperature, °C

$\bar{T}_g$ – mean gas temperature over the row thickness, °C

T_s – steam temperature, °C

T_w – tube wall temperature, °C

w – steam velocity, m/s

x^+ – dimensionless coordinate in the steam flow direction

y^+ – dimensionless coordinate in the flue gas flow direction

Greek symbols

δ_a – thickness of ash deposits, m

δ_s – thickness of iron oxide or scale deposits, m

ϕ – angle between tube axis and horizontal plane, m

ρ – steam density, kg/m³

ξ – friction factor

1 Introduction

Superheaters are tubular cross-flow heat exchangers, however, they differ very significantly from the other heat exchangers operating at moderate temperatures. The characteristic feature of superheaters is a complicated flow arrangement and high steam and flue gas temperature (Fig. 1). Because of the strong dependence of the steam specific heat on pressure and tem-
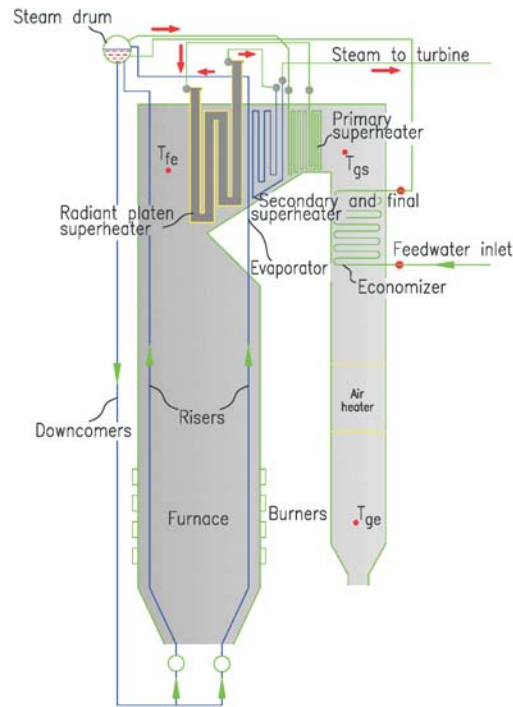
Figure 1. Coal-fired utility boiler with natural circulation: T_{fe}, T_{gs}, and T_{ge} denote flue gas temperatures at the furnace exit, after the superheaters and after the air heater, respectively.

perature, the superheater cannot be calculated using conventional methods such as a number of transfer units method or the method based on the mean logarithmic temperature difference between the fluids [1–3].

Correct design of the boiler superheater is very difficult. This results, on one hand, from the complexity of heat transfer by radiation of flue gas with a high content of solid ash particles, and on the other hand, from the fouling of heating surfaces by slag and ash [4–8]. The degree of the slag and ash deposition is hard to assess, both at the design stage and during the boiler operation. In consequence, the proper size of superheaters is being assumed only after boiler starting. In cases when the temperature of superheated steam at the exit from the superheater stage under examination is higher than the design value, then the area of the surface of this stage has to be decreased. However, if the exit temperature of the steam is below the desired value, then the surface area is increased.

Due to the high cost of steel alloys each superheater stage is usually made of different steel. Detailed calculation of superheater tube wall temperature is very important. The steel grade can be properly selected to avoid overheating of the superheater tubes during the boiler operation if the tube wall temperature is known along the flow path of the water steam.

Superheaters and reheaters are the tube bundles that achieve the highest temperatures in a boiler and therefore require the greatest attention in the design, fabrication, operation and maintenance to ensure that the allowable metal temperatures are never exceeded [9]. A standard method for hydraulic and thermal calculations of steam boilers, including steam superheaters, is presented in [4–6]. Although the boiler standards are widely used by manufacturers of boilers, they adopt for the calculation of the superheaters procedures which are used in design or performance calculations of common heat exchangers assuming constant physical fluid properties. The basic superheater and reheater design principles are discussed in detail by Rayaprolu [10]. Design and performance procedures for calculating of coal fired boilers were described. Much attention has been paid for analyzing start-ups of steam boilers. Approximately 40% of all boiler failures are caused by damage of steam superheaters due to overheating of the material [11]. For this reason, steam superheaters are modeled mathematically or monitored to avoid overheating of tubes. Simulations and optimization results of a 300 MW lignite-fired power boiler are presented by Tzolakis *et al.* [12].

A heat recovery steam generator (HRSG) was optimized by Behbahaninia using the genetic algorithm [13]. The results show that the thermodynamic optimization is not capable to decrease significantly the total cost of the HRSG. Mathematical modeling of the boiler superheater is the subject of few publications in spite of great practical significance of the problem. This is mainly due to the difficulty of the description of complex flow and heat transfer phenomena occurring in the steam superheaters both in pulverized coal and fluidized boilers. A lot of trouble makes the flue gas temperature non-uniformity in the channel cross-section, in which the superheater is located. A thermal load deviation model for the superheater and reheater of a utility boiler was developed by Xu *et al.* [14]. Many failure analyses on the superheaters were carried out to reveal the causes of tube overheating or tube rapture. The steam temperature deviation is one of the fundamental causes of boiler tube failures. The 320 MW natural gas fired boiler was modeled using the CFD code by Rahimi *et al.* [15]. The main aim of the numerical analysis was to find the reason for the tube rupture

inside the boiler. A new method for estimating heat flux in superheater and reheater tubes based on the empirical formulas and the finite element modeling is presented by Purbolaksono *et al.* [16].

The finite element analyses were performed by Othman *et al.* [17] to identify the possible root cause failure of the deformed superheater tubes. It was found that temperature was the main factor of the deformation due to restriction to the tube. Local short-term overheating of the tubes due to concentrated flue gas flow resulted in a failure of the primary superheater tubes [18]. A failure analysis was conducted using visual inspections, in situ measurements of hardness and finite element analyses. The rate of corrosive wear in superheaters of supercritical boilers was studied in the paper by Pronobis and Wojnar [19]. The slagging and fouling phenomena in superheaters impact the boiler efficiency and lifetime. Harding and O'Connor used the ten-year database to determine the lost generation through either forced outages and forced the rates due to coal quality or slagging and fouling issues [20]. A computer system for monitoring slagging and fouling of superheaters is described in [7].

The review of literature shows that previous papers on the superheaters are mostly experimental and relate to search for the causes of failures of superheater tubes or analyze ash fouling. In most cases, the microstructure of the overheated tube wall material is examined and strength calculations are carried out using commercial software based on the finite element method. In order to detect the causes of failures, an analysis of thermal flow processes occurring in the boiler superheaters is required.

In this paper a numerical method for superheater modeling is developed. Flow and heat transfer processes in cross-flow tube heat exchangers with complex flow arrangements can be modeled. The method allows the modeling of superheaters with ash buildups on the tubes. Much attention will be paid to assessing the impact of scale deposits on the internal tube surfaces on steam and tube wall distributions. A detailed analysis of the impact of flue gas temperature unevenness across the width of the superheater on the temperature of steam and superheater tubes will be conducted. Considering that the steam flows in parallel through many tubes, nonuniformity of the flue gas temperature also causes the changes of the steam mass flow rates through individual steam superheater tubes, which in turn increases the difference in steam temperature at the outlet of the superheater tubes. This is a dangerous phenomenon often causing permanent deformation of superheater outlet headers, leading to shortened lifetime of the superheater

tubes and outlet headers. Ash deposits on the flue gas side is also be taken
into account. A new procedure for determining thermal resistance of an ash
deposit on the superheater surface is presented.

2   Mathematical model of the superheater

A basis for the mathematical model of a steam superheater with a complex
tube arrangement (Fig. 2) is the heat transfer model for the single tube
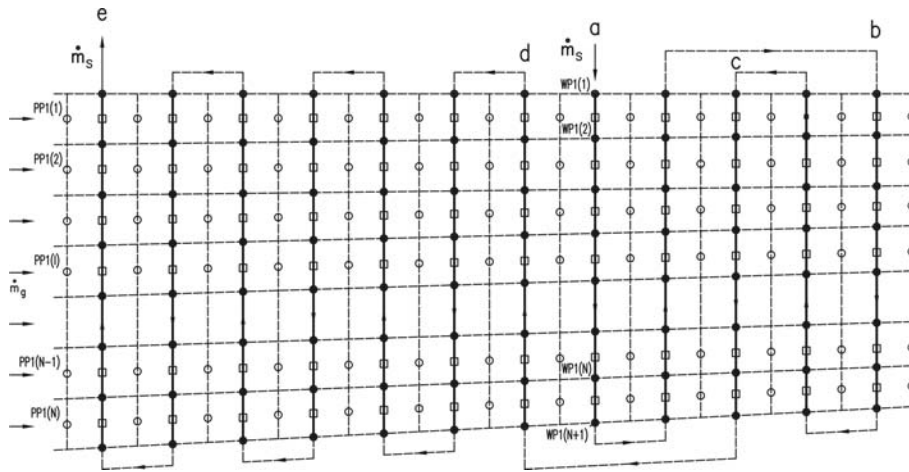placed in a one-row cross flow tube heat exchanger (Fig. 3).

Figure 2. Superheater flow arrangement and division of superheater into control volumes:
o – flue gas, ● – water steam, □ – tube wall; PP1(1), ...,PP1(N) – flue gas
temperature at the nodes before the superheater, WP1(1),..., WP1(N+1) –
steam temperature at the nodes in the first superheater pass.

The governing partial differential equations describing the space and
time changes of steam, T_s, tube wall, T_w, deposit layer, T_a, and flue gas T_g,
temperatures are:

$$\frac{1}{N_s} \frac{\partial T_s}{\partial x^+} + (T_s - T_w |_{r=r_{in}}) = 0 , \qquad 0 \leq x^+ \leq 1 , \tag{1}$$

$$\frac{1}{r} \frac{\partial}{\partial r} \left(r \, k_w \frac{\partial T_w}{\partial r} \right) = 0 , \qquad r_{in} \leq r_w \leq r_o , \tag{2}$$

$$\frac{1}{r} \frac{\partial}{\partial r} \left(r \, k_a \frac{\partial T_a}{\partial r} \right) = 0 , \qquad r_o \leq r \leq r_a , \tag{3}$$
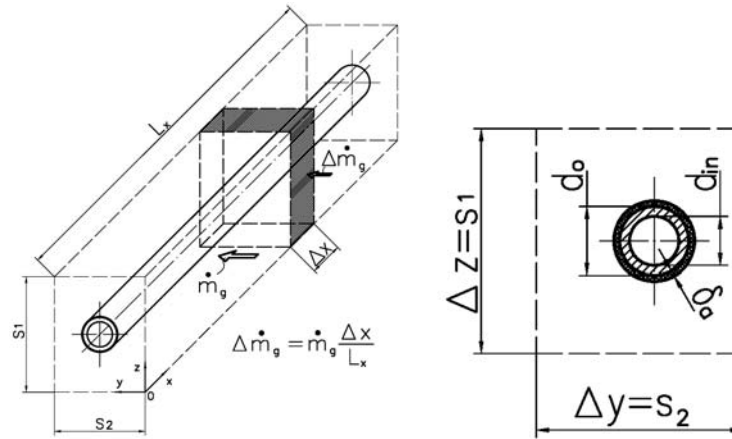
Figure 3. Single superheater tube; water steam flows inside the tube, and flue gas flows
perpendicular to the tube axis.

$$\frac{1}{N_g}\frac{\partial T_g}{\partial y^+} + (T_g - T_w\,|_{r=r_a}) = 0 \,, \qquad 0 \leq y^+ \leq 1 \,. \tag{4}$$

The numbers of heat transfer units N_s and N_g are given by

$$N_s = \frac{h_s\,A_{in}}{\dot{m}_s\,c_{ps}} \,, \quad N_g = \frac{h_g\,A_a}{\dot{m}_g\,c_{pg}} \,. \tag{5}$$

The symbols in Eqs. (1)–(5) denote: $x^+ = x/L_r$ and $y^+ = y/s_2$ – dimensionless coordinate in the steam and flue gas flow directions, L_r – tube length, s_2 – transversal pitch of tubes, r – radius, r_{in} and r_o – inner and outer tube radius, r_a – outer radius of deposit layer, k_w and k_a – tube material and ash deposit thermal conductivity.

The energy balance equations (1) and (4) are subject to the following boundary conditions at the inlets of the steam superheater

$$T_s\left(x^+\right)\,|_{x^+=0} = f_1 \,, \tag{6}$$

$$T_g\left(y^+\right)\,|_{y^+=0} = f_2 \,, \tag{7}$$

where the symbols f_1 and f_2 stand for the inlet steam and flue gas temperature, respectively.

The convective boundary conditions for the tube covered by ash deposits are

$$\left(k_w\frac{\partial T_w}{\partial r}\right)\Big|_{r=r_{in}} = h_s\left(T_w\big|_{r=r_{in}} - T_s\right) \,, \tag{8}$$

$$\left(k_a \frac{\partial T_a}{\partial r} \right) \bigg|_{r=r_a} = h_g \left(\bar{T}_g - T_a \big|_{r=r_a} \right) , \tag{9}$$

where the symbol $\bar{T}_g$ (Fig. 4) stands for the mean gas temperature over the row thickness, defined as

$$\bar{T}_g = \int_0^1 T_g \left(x^+, y^+ \right) dy^+ . \tag{10}$$

The symbol h_s denotes the heat transfer coefficient at the inner tube surface and h_g the heat transfer coefficient on the flue gas side.
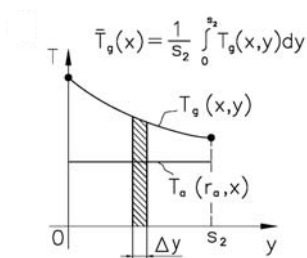

Figure 4. Determining of the mean flue gas temperature over a tube row (over pitch s_2).

At the contact interface between the tube and deposit layer the temperature and heat flux are the same

$$T_w|_{r=r_o} = T_a|_{r=r_o} , \tag{11}$$

$$\left(k_w \frac{\partial T_w}{\partial r} \right) \bigg|_{r=r_o} = \left(k_a \frac{\partial T_a}{\partial r} \right) \bigg|_{r=r_o} . \tag{12}$$

Ash deposits on externals surfaces reduce slightly tube wall temperatures. The impact of steam-side scale deposits is reversed. Due to the low thermal conductivity, the temperature increase over the scale layer is high. This leads to a higher tube wall temperature which in turn reduces the stress rapture life considerably. To simplify the analysis, the steam-side oxide scale is considered to be a single-layered oxide deposit of uniform thickness δ_s. The presence of iron oxides with the thermal conductivity k_s on the inner surfaces of superheater tubes will be taken into account by introducing an equivalent heat transfer coefficient h_e defined as

$$\frac{1}{h_e} = \frac{r_{in}}{k_s} \ln \frac{r_{in}}{r_{in} - \delta_s} + \frac{r_{in}}{r_{in} - \delta_s} \frac{1}{h_s} . \tag{13}$$

When the inner tube surfaces are fouled with scales, then in place of the heat transfer coefficient h_s for clean surfaces in Eq. (8) we have to insert the equivalent heat transfer coefficient.

The finite volume method (FVM) was used to solve the system of differential equations for temperature of the both fluids and the tube wall with appropriate boundary conditions. A numerical model of multi-pass steam superheater with twelve tube rows (passes) (Fig. 2) was developed. The location of the superheater in the boiler is shown in Fig. 1. The convection and radiation heat transfer on the flue gas side was accounted for. In addition, the deposit layers will be assumed to cover the inner and outer surfaces of the tubes.

At first a model of the superheater is divided into finite control volumes. As an example of the superheater stage, the first stage convective superheater will be considered. The flow arrangement and division of this superheater stage into finite volumes is depicted in Fig. 2. The superheated steam and the combustion products flow at right angles to each other. The first stage convective superheater can be classified according to flow arrangement as a mixed-cross-flow heat exchanger. The superheater tubes are arranged in-line. Each individual pass consists of two tubes through which superheated steam flows parallel. In the following, finite volume heat balance equations will be formulated for the steam, tube wall, and flue gas.

A basis for the formulating of the mathematical model of the whole superheater is a single tube placed in a cross-flow. Tubes are arranged in an in line tube bundle. The tube arrangement in the superheater is characterized by the longitudinal pitch s_2 parallel to the flu gas flow direction and the pitch s_1, perpendicular to the flue gas flow direction (Fig. 3). The tube cross-flow heat exchanger consisting of separate tubes will be replaced by a continuous heat exchanger with a heat transfer surface extending over the entire pitch s_2 (Figs. 3–5).

3   Heat balance equations for steam

A steam side energy balance equation for the ith finite volume with dimensions $s_1 \times s_2 \times \Delta x$ (Figs. 3 and 5) gives

$$\dot{m}_s \; c_{ps}\big|_0^{T_{s,i}} \; T_{s,i} + \pi \, d_{in} \, \Delta x \, h_s \left(T_{w1,i} - \frac{T_{s,i} + T_{s,i+1}}{2} \right) = \dot{m}_s \; c_{ps}\big|_0^{T_{s,i+1}} \, T_{s,i+1} \, , \tag{14}$$
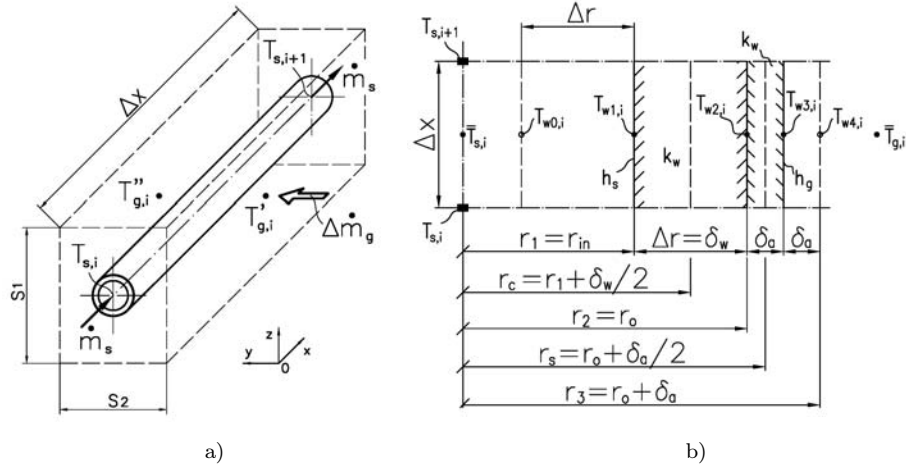
Figure 5. Finite volumes for the steam and flue gas (a) and for tube wall (b).

where the symbol $c_{ps}|_0^{T_s}$ denotes the mean specific heat at constant pressure p in the temperature interval $[0,T_s]$.

Introducing the mean specific heat defined as

$$\bar{c}_{ps,i} = c_{ps}|_{T_{s,i}}^{T_{s,i+1}} = \frac{c_{ps}|_0^{T_{s,i+1}} T_{s,i+1} - c_{ps}|_0^{T_{p,i}} T_{s,i}}{T_{s,i+1} - T_{s,i}} \simeq \frac{c_{ps}(T_{s,i}) + c_{ps}(T_{s,i+1})}{2} \ . \tag{15}$$

Equation (14) can be transformed to the following form

$$\dot{m}_s\,\bar{c}_{ps,i}\,(T_{s,i+1} - T_{s,i}) = \Delta A_{in}\,h_s\left(T_{w1,i} - \frac{T_{s,i} + T_{s,i+1}}{2}\right)\,, \tag{16}$$

where $\Delta A_{in} = \pi\,d_{in}\,\Delta x$. The length of the finite volume is $\Delta x = L_x/N$, where N is the number of finite volumes on the tube length.
Solving Eq. (16) for $T_{s,i+1}$ yields

$$T_{s,i+1} = \frac{h_s\,\Delta A_{in}\,T_{w1,i} + T_{s,i}\left(\dot{m}_s\,\bar{c}_{ps,i} - \frac{1}{2}\,h_s\,\Delta A_{in}\right)}{\dot{m}_s\,\bar{c}_{ps,i} + \frac{1}{2}\,h_s\,\Delta A_{in}},\quad i = 1,\dots,N\ . \tag{17}$$

After introducing the mesh number of transfer units for the steam

$$\Delta N_{s,i+\frac{1}{2}} = \frac{h_s\,\Delta A_{in}}{\dot{m}_s\,\bar{c}_{ps,i}} = \frac{2\,h_s\,\Delta A_{in}}{\dot{m}_s\left[c_{ps}(T_{s,i}) + c_{ps}(T_{s,i+1})\right]}\,, \tag{18}$$

Eq. (17) can be rewritten in the form

$$T_{s,i+1} = \frac{1}{1 + \frac{1}{2}\,\Delta N_{s,i+\frac{1}{2}}} \left[\left(1 - \frac{1}{2}\,\Delta N_{s,i+\frac{1}{2}}\right) T_{s,i} + \Delta N_{s,i+\frac{1}{2}}\,T_{w1,i} \right],$$
$$i = 1,\ldots, N . \quad (19)$$

The system of algebraic equations (17) is written in a form suitable for applying the iterative method of Gauss-Seidel to solve it.

4 Heat balance equations for tube wall covered with ash deposits

Next, heat balance equations will be formulated for the nodes shown in Fig. 5b. The nodes are located at the inner and outer radius of the tube and outer deposit surface. Temperature dependent physical properties of the tube material and ash deposits were assumed. The boundary condition at the inner surface given by Eq. (8) is approximated as follows

$$k\,(T_{w1,i})\,\frac{T_{w2,i} - T_{w0,i}}{2\,\Delta r} = h_s\,\left(T_{w1,i} - \bar{T}_{s,i}\right), \quad i = 1,\ldots, N . \quad (20)$$

The space derivative of the temperature in Eq. (8) was replaced by the central differential quotient of second-order accuracy. In consequence, the imaginary node **0** was introduced (Fig. 5b). Solving Eq. (20) for the temperature $T_{w0,i}$ at the imaginary node gives

$$T_{w0,i} = T_{w2,i} - \frac{2\,h_s\,\Delta r}{k\,(T_{w1,i})}\,\left(T_{w1,i} - \bar{T}_{s,i}\right), \quad i = 1,\ldots, N . \quad (21)$$

The heat balance equation for the node **1** is

$$\left(1 - \frac{\Delta r}{2\,r_1}\right) \frac{k_{w\,0,i} + k_{w\,1,i}}{2\,k_{w\,1,i}}\,(T_{w\,0,i} - T_{w\,1,i}) +$$
$$\left(1 + \frac{\Delta r}{2r_1}\right) \frac{k_{w\,2,i} + k_{w\,1,i}}{2k_{w\,1,i}}\,(T_{w1,i} - T_{w\,2,i}) = 0 , \quad i = 1,\ldots, N . \quad (22)$$

This equation is transformed into the form, which is suitable for the solution of the equation system by the Gauss-Seidel method

$$T_{w\,1,i} = \frac{\left(1 - \frac{\Delta r}{2r_1}\right) T_{w0,i} + \left(1 + \frac{\Delta r}{2r_1}\right) \frac{k_{w\,2,i} + k_{w\,1,i}}{k_{w\,0,i} + k_{w\,1,i}} T_{w\,2,i}}{\left(1 - \frac{\Delta r}{2r_1}\right) + \left(1 + \frac{\Delta r}{2r_1}\right) \frac{k_{w\,2,i} + k_{w\,1,i}}{k_{w\,0,i} + k_{w\,1,i}}} , \quad i = 1,\ldots, N .$$
$$(23)$$

The heat balance equation for the node **2** (Fig. 5b) located at the interface between the tube and the deposits has the following form

$$\left(1 - \frac{\delta_w}{2\,r_2}\right)\frac{k_{w\,1,i} + k_{w\,2,i}}{2\,k_{w\,2,i}}\left(T_{w\,1,i} - T_{w\,2,i}\right) +$$
$$\left(1 + \frac{\delta_a}{2\,r_2}\right)\frac{k_{a\,3,i} + k_{w\,2,i}}{2\,k_{w\,2,i}}\left(T_{w\,3,i} - T_{w\,2,i}\right) = 0\,, \quad i = 1, \ldots, N\,. \qquad (24)$$

Solving Eq. (24) for $T_{w\,2,i}$ yields

$$T_{w\,2,i} = \frac{\left(1 - \frac{\delta_w}{2r_2}\right)\frac{k_{w\,1,i} + k_{w\,2,i}}{2}\frac{T_{w\,1,i}}{\delta_w} + \left(1 + \frac{\delta_a}{2r_2}\right)\frac{k_{w\,2,i} + k_{a\,3,i}}{2}\frac{T_{w\,3,i}}{\delta_a}}{\left(1 - \frac{\delta_w}{2r_2}\right)\frac{k_{w\,1,i} + k_{w\,2,i}}{2}\frac{1}{\delta_w} + \left(1 + \frac{\delta_a}{2r_2}\right)\frac{k_{w\,2,i} + k_{a\,3,i}}{2}\frac{1}{\delta_a}}\,,$$
$$i = 1, \ldots, N\,. \qquad (25)$$

Approximating the boundary condition (9) using the central difference quotient

$$k_a\left(T_{w\,3,i}\right)\frac{T_{w\,4,i} - T_{w\,2,i}}{2\,\delta_a} = h_g\left(\bar{T}_{g,i} - T_{w\,3,i}\right)\,, \quad i = 1, \ldots, N \qquad (26)$$

the temperature $T_{w\,4,i}$ at the imaginary node **4** can be determined

$$T_{w\,4,i} = T_{w\,2,i} + \frac{2\,h_g\,\delta_a}{k_a\left(T_{w\,3,i}\right)}\left(\bar{T}_{g,i} - T_{w\,3,i}\right)\,, \quad i = 1, \ldots, N\,. \qquad (27)$$

From the heat balance equation for the node **3**

$$\left(1 - \frac{\delta_a}{2r_3}\right)\frac{k_{a\,2,i} + k_{a\,3,i}}{2\,k_{a\,3,i}}\left(T_{w\,2,i} - T_{w\,3,i}\right) +$$
$$\left(1 + \frac{\delta_a}{2r_3}\right)\frac{k_{a\,3,i} + k_{a\,4,i}}{2\,k_{a\,3,i}}\left(T_{w\,4,i} - T_{w\,3,i}\right) = 0\,, \quad i = 1, \ldots, N \qquad (28)$$

one obtains

$$T_{w\,3,i} = \frac{\left(1 - \frac{\delta_a}{2r_3}\right)\frac{k_{a\,2,i} + k_{a\,3,i}}{2\,k_{a\,3,i}}T_{w\,2,i} + \left(1 + \frac{\delta_a}{2r_3}\right)\frac{k_{a\,3,i} + k_{a\,4,i}}{2\,k_{a\,3,i}}T_{w\,4,i}}{\left(1 - \frac{\delta_a}{2r_3}\right)\frac{k_{a\,2,i} + k_{a\,3,i}}{2\,k_{a\,3,i}} + \left(1 + \frac{\delta_a}{2r_3}\right)\frac{k_{a\,3,i} + k_{a\,4,i}}{2\,k_{a\,3,i}}}\,,$$
$$i = 1, \ldots, N\,. \qquad (29)$$

If the thermal conductivity of the tube material and deposit layer are constant, then equations: (21), (23), (25), (27), and (29) can be simplified to

the following linear equation set

$$T_{w1,i} = \frac{(2r_1 - \delta_w)\,h_s\,\bar{T}_{s,i} + \frac{2r_1\,k_w}{\delta_w}T_{w\,2,i}}{\frac{2k_w r_1}{\delta_w} + (2r_1 - \delta_w)\,h_s} \ , \quad i = 1,\ldots,N \ , \qquad (30)$$

$$T_{w\,2,i} = \frac{\left(1 - \frac{\delta_w}{2r_2}\right)\frac{k_w}{\delta_w}T_{w\,1,i} + \left(1 + \frac{\delta_a}{2r_2}\right)\frac{k_w + k_a}{2\,\delta_a}T_{w\,3,i}}{\left(1 - \frac{\delta_w}{2r_2}\right)\frac{k_w}{\delta_w} + \left(1 + \frac{\delta_a}{2r_2}\right)\frac{k_w + k_a}{2\delta_a}} \ , \quad i = 1,\ldots,N \ ,$$

$$(31)$$

$$T_{w\,3,i} = \frac{T_{w\,2,i} + \frac{h_g\,\delta_a}{k_a}\left(1 + \frac{\delta_a}{2r_3}\right)\bar{T}_{g,i}}{1 + \frac{h_g\,\delta_a}{k_a}\left(1 + \frac{\delta_a}{2r_3}\right)} \ , \quad i = 1,\ldots,N \ . \qquad (32)$$

The mean steam temperature $\bar{T}_{s,i}$ and mean gas temperature $\bar{T}_{g,i}$ are defined as follows (Fig. 5):

$$\bar{T}_{s,i} = \frac{T_{s,i} + T_{s,i+1}}{2} \ \text{ and } \ \bar{T}_{g,i} = \frac{T'_{g,i} + T''_{g,i}}{2} \ , \quad i = 1,\ldots,N \ , \qquad (33)$$

The average temperature of the steam and gas over the area of one cell was calculated using the arithmetic mean since the steam and flue gas temperature changes within the cell are small.

5   Heat balance equations for flue gas

Heat balance equation for the finite volume shown in Fig. 5a is

$$\Delta\dot{m}_g\ c_{pg}|_0^{T'_{g,i}}\ T'_{g,i} = \Delta\dot{m}_g\ c_{pg}|_0^{T''_{g,i}}\ T''_{g,i} +$$
$$\pi\,(2\,r_o + 2\,\delta_a)\,\Delta x\,h_g\left(\frac{T'_{g,i} + T''_{g,i}}{2} - T_{w\,3,i}\right) \ , \quad i = 1,\ldots,N \ . \qquad (34)$$

Introducing the mean specific heat defined as

$$c_{pg}\Big|_{T''_{g,i}}^{T'_{g,i}} = \frac{c_{pg}|_0^{T'_{g,i}}\ T'_{g,i} - c_{pg}|_0^{T''_{g,i}}\ T''_{g,i}}{T'_{g,i} - T''_{g,i}} \cong \bar{c}_{pg,i}, \quad i = 1,\ldots,N \qquad (35)$$

we can transform the energy balance, Eq. (14), to the following form

$$\Delta\dot{m}_g\,\bar{c}_{pg,i}\left(T'_{g,i} - T''_{g,i}\right) = \Delta A_a\,h_g\left(\frac{T'_{g,i} + T''_{g,i}}{2} - T_{w\,3,i}\right) \ , \quad i = 1,\ldots,N \ ,$$

$$(36)$$

where $\Delta A_a = \pi \left(2\, r_o + 2\, \delta_a \right) \Delta x$.

Solving Eq. (36) for $T''_{g,i}$ yields

$$T''_{g,i} = \frac{\left(\Delta \dot{m}_g\, \bar{c}_{pg,i} - \frac{1}{2}\, h_g \Delta A_a \right) T'_{g,i} + h_g\, \Delta A_a\, T_{w\,3,i}}{\Delta \dot{m}_g\, \bar{c}_{pg,i} + \frac{1}{2}\, h_g\, \Delta A_a} \; . \tag{37}$$

After introducing the mesh number of transfer units for the flue gas

$$\Delta N_{g,i+\frac{1}{2}} = \frac{h_g\, \Delta A_a}{\Delta \dot{m}_g\, \bar{c}_{pg,i}} = \frac{2\, h_g\, \Delta A_a}{\Delta \dot{m}_g \left[c_{pg}\left(T'_{g,i} \right) + c_{pg}\left(T''_{g,i} \right) \right]} \; ,$$
$$i = 1, \dots, N \; . \tag{38}$$

Equation (37) can be written in the form

$$T''_{g,i} = \frac{1}{1 + \frac{1}{2}\, \Delta N_{g,i+\frac{1}{2}}} \left[\left(1 - \frac{1}{2}\, \Delta N_{g,i+\frac{1}{2}} \right) T'_{g,i} + \Delta N_{g,i+\frac{1}{2}}\, T_{w3,i} \right] \; ,$$
$$i = 1, \dots, N \; . \tag{39}$$

To determine the temperature of the steam, tube wall and flue gas the equation set: (19), (21), (23), (25), (27), (29), and (39) was solved using the Gauss-Seidel method.

The convective heat transfer coefficient at the tube inner surface, h_s, and the heat transfer on the flue gas side, h_{cg}, were calculated using correlations given in [5,6]. Experimental correlations presented in [1,21] can also be applied to calculate heat transfer coefficient in cross-flow tube bundles. The effect of radiation on the heat transfer coefficient, h_g, is accounted for by adding the radiation heat transfer coefficient, h_{rg}, [5,8] to the convective heat transfer, e.g.,

$$h_g = h_{cg} + h_{rg} \; . \tag{40}$$

The changes of pressure along the steam flow path are determined from the momentum conservation equation for the steady state [1,4]. The momentum conservation equation for one-dimensional steady flow has the following form:

$$\frac{d\,p}{d\,s} = -\rho w \frac{d\,w}{d\,s} - \rho g \sin \phi - \frac{\xi}{d_h} \rho \frac{w\,|w|}{2} \; , \tag{41}$$

where p – static pressure, s – coordinate along the flow path in direction of flow, w – steam velocity, ρ – steam density, ϕ – angle between tube axis and horizontal plane, ξ – Darcy–Weisbach friction factor, d_h – hydraulic

diameter of the superheater tube (for a circular tube, this equals the inner diameter of the tube). Equation (41) was solved by finite differences for known inlet pressure, p_{in}, and steam mas flow rate, $\dot{m}_s$. The temperature distribution along the steam flow path was obtained using the thermal model of the heat exchanger presented above.

6   Example of calculation of the superheater with scale deposits on the inner surfaces of the tubes

The calculations were performed for the first stage of convection super-heater installed in the steam boiler OP-210 with a capacity of 210×10^3 kg/h. The parameters of live steam are: pressure $p = 9.61$ MPa, and temperature $T = 532.8$ °C. The flow arrangement and division of the first stage convective superheater into finite volumes is depicted in Fig. 5. The superheated steam and the combustion products flow at right angles to each other. The first stage convective superheater can be classified according to flow arrangement as a mixed-cross-flow heat exchanger with twelve passes (Fig. 2). The superheater tubes are arranged in-line. Each individual pass consists of two tubes through which superheated steam flows parallel. In the entire superheater steam flows parallel through 148 tubes.

The steam temperature at the inlet of the superheater was of 318.7 °C and the inlet flue gas temperature was of 882.1 °C. The superheater tubes are made of Russian Steel grade 20. The inner radius of the tubes was $r_{in} = 16$ mm and the tube thickness was of 5 mm. The tube inner surface is covered with a layer of scale deposits. The thermal conductivity of the steel is given by the following expression

$$k_w = 51.7465 - 0.006704\,T - 4.19 \cdot 10^{-05}\,T^2 \; , \qquad (42)$$

where k_w is in W/(m K) and T in °C.

In order to show the effect of internal scale deposits on the heat flow rate transferred from the flue gas to the steam, and the temperature of the superheater tubes the following data have been adopted for the calculation: $\delta_a = 0$ m, $\delta_s = 0.0005$ m, $k_s = 0.15$ W/(m K). The heat transfer coefficient at the inner surface of the clean tube is $h_s = 2283.1$ W/(m^{2}K) while for the fouled tubes is larger and equal to $h_s = 2589.5$ W/(m^{2}K), since the steam velocity increases due to the smaller inner diameter of the tube with a layer of scales. The equivalent heat transfer coefficient defined by Eq. (13) is $h_e = 264.2$ W/(m^{2}K).

The results of the numerical simulations are shown in Figs. 6 and 7. An inspection of the results depicted in Fig. 6 indicates that the internal scales have a large impact on the steam temperature. For the superheater with fouled tubes the steam temperature at the outlet of the superheater is about 25 K lower compared to the superheater with clean tubes. Maximum tube wall temperature in superheater with scale deposits is $T_w = 528.2$ °C while for the superheater without scale deposits is $T_w = 465.2$ °C.
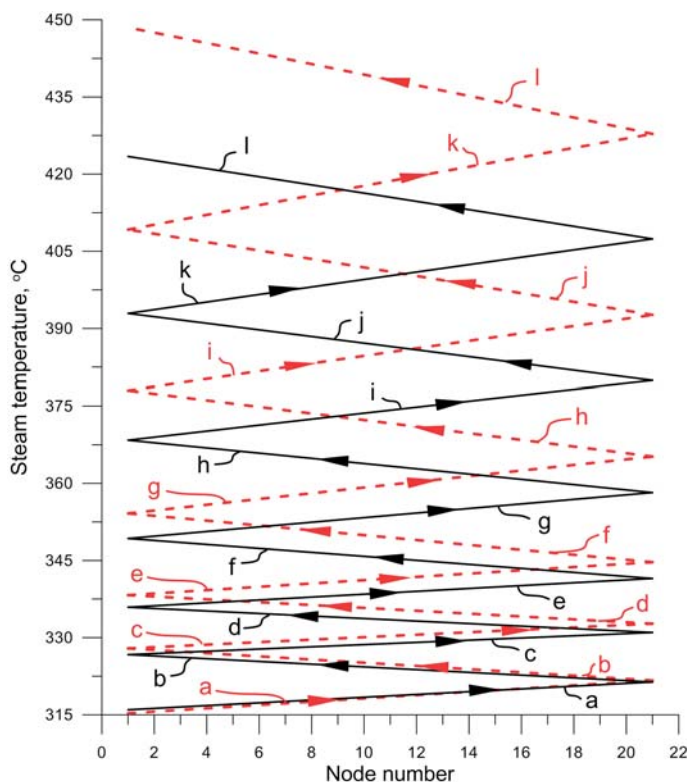

Figure 6. Steam temperature changes along the steam flow path for clean (red dashed line) and fouled (black solid line) inner surfaces of the superheater tubes.

The heat flow rate transferred from the flue gas to the steam is equal to $\dot{Q}_c = 3.3394$ MW for the clean superheater and for the fouled superheater drops to $\dot{Q}_f = 2.8201$ MW. The relative decline in the superheater output, defined as $100 \left(\dot{Q}_c - \dot{Q}_f \right) / \dot{Q}_c$, is equal to 15.55%. This example shows the harmful effects of internal scale deposits on the operation conditions of the

superheater. The heat flow rate decreases while increasing the maximum
temperature of the metal, which in turn can lead to overheating of the tube
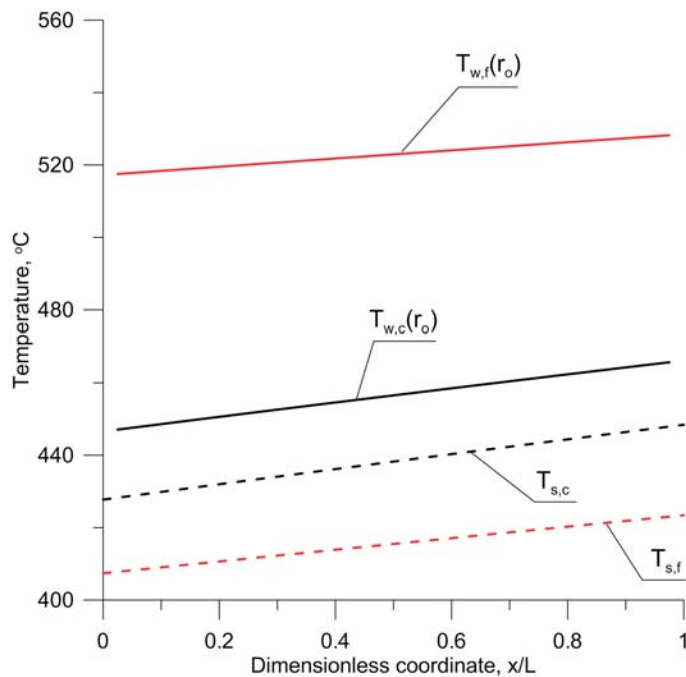material.

Figure 7. Steam and tube wall temperature changes along the steam flow path in the
tube L for the clean and fouled inner surfaces of the superheater tubes; $T_{s,c}$ and
$T_{w,c}(r_o)$ – steam and tube wall temperature for clean tube, $T_{s,f}$, and $T_{w,f}(r_o)$
– steam and tube wall temperature for tube with fouled inner surface.

7   Conclusions

The developed modeling technique can especially be used for modeling
boiler superheaters when detailed information on the tube wall tempera-
ture distribution is needed. The method of modeling the superheater can
be used both in the design, as well as in upgrading the superheaters. If
the steam temperature at the outlet of the superheater is too low or too
high, the designed outlet temperature can be achieved by changing a flow
arrangement of the superheater. For example, the impact of the change of
the counter to parallel flow or to mixed flow can be easily assessed. The

presented method of modeling is a useful tool in analyzing the impact of the internal scales or outer ash fouling on the superheater operating conditions.

Received 14 October 2013

References

[1] HEWITT G.F., SHIRES G.L., BOTT T.R.: *Process Heat Transfer.* CRC Press – Begell House, Boca Raton, 1994.

[2] SHAH R.K., SEKULIĆ D.P.: *Fundamentals of heat exchanger design.* Wiley, Hoboken, 2003.

[3] KAKAÇ S., LIU H.: *Heat Exchangers: Selection, Rating, and Thermal Design*, 2nd Edn. CRC Press-Taylor & Francis Group, Boca Raton, 2002.

[4] LOKSHIN V.A., PETERSON D.F., SCHWARZ A.L.: *Standard Methods of Hydraulic Design for Power Boilers.* Hemisphere Publishing Corporation, Washington – New York – London, 1998.

[5] KUZNETSOV N.W., MITOR W.W., DUBOVSKI I.E., KARASINAE.S. (EDS.): *Thermal Calculations of Steam Boilers (Standard Method)*, 2nd Edn. Energia, Moscow 1973, Russia.

[6] LIN Z.H.: *Thermo-hydraulic design of fossil-fuel-fired boiler components.* In: , *Boilers, Evaporators, and Condensers* (S. Kakaç, Ed.), John Wiley & Sons Inc., Hoboken, 1991, 363–469.

[7] TALER J., TROJAN M., TALER D.: *Monitoring of Ash Fouling and Internal Scale Deposits in Pulverized Coal Fired Boilers.* Nova Science Publishers Inc., New York 2011.

[8] TALER D., TALER J.: *Simplified analysis of radiation heat exchange in boiler superheaters.* Heat Trans. Eng. **30**(2009), 661–669.

[9] LUDOWSKI P., TALER D., TALER J.: *Identification of thermal boundary conditions in heat exchangers of fluidized bed boilers.* Appl. Therm. Eng. **58**(2013), 194–204.

[10] RAYAPROLU K.: *Boiler for Power and Process.* CRC Press – Taylor & Francis Group, Boca – Raton 2009.

[11] FRENCH D.N.: *Metallurgical failures in fossil fired boilers.* 2nd Edn. John Wiley & Sons, New York 1993.

[12] Tzolakis G., Papanikolaou P., Kolokotronis D., Samaras N., Tourlidakis A., Tomboulides A.: *Simulation of a coal-fired power plant using mathematical programming algorithms in order to optimize its efficiency.* Appl. Therm. Eng. **48**(2012) 256–267.

[13] Behbahaninia A., Bagheri M., Bahrampoury R.: *Optimization of the fire tube heat recovery steam generators for cogeneration plants through genetic algorithm.* Appl. Therm. Eng. **30**(2010), 2378–2385.

[14] Xu L., Khan J.A., Chen Z.: *Thermal load deviation model for superheater and reheater of a utility boiler.* Appl. Therm. Eng. **20**(2000), 545–558.

[15] Rahimi M., Khoshhal A., Shariati S.M.: *CFD modeling of a boiler's tubes rupture.* Appl. Therm. Eng. **26**(2006) 2192–2200.

[16] Purbolaksono J., Khinani A., Rashid A.Z., Ali A.A., Ahmad J., Nordin N.F.: *A new method for estimating heat flux in superheater and reheater tubes.* Nucl. Eng. Design **239**(2009), 1879–1884.

[17] Othman H., Purbolaksono J., Ahmad B.: *Failure investigation on deformed superheater tubes.* Eng. Failure Anal. **16**(2009), 329-339.

[18] Purbolaksono J., Ahmad J., Beng L.C., Rashid A.Z., Khinani A., Ali A.A.: *Failure analysis on a primary superheater tube of a power plant.* Eng. Failure Anal. **17**(2010), 158–167.

[19] Pronobis M., Wojnar W.: *The rate of corrosive wear in superheaters of boilers for supercritical parameters of steam.* Eng. Failure Anal. **19**(2012), 1–12.

[20] Harding N.S., O'Connor D.C.: *Ash deposition impacts in the power industry.* Fuel Proces. Techn. **88**(2007), 1082–1093.

[21] Gnielinski V.: *Heat transfer in cross-flow around single rows of tubes through tube bundles*, 2nd Edn. In: VDI Heat Atlas, Springer, Berlin-Heidelberg 2010, G7, 725–730.